Available online at www.sciencedirect.com
SciVerse ScienceDirect
Ceramics International 39 (2013) 871–876
CERAMICS INTERNATIONAL
www.elsevier.com/locate/ceramint

Short communication

Improving high temperature properties of hot pressed ZrB_2–20 vol% SiC ceramic using high purity powders

Ji Zou[a,b], Guo-Jun Zhang[b,*], Hui Zhang[b], Zheng-Ren Huang[b], Jef Vleugels[a,*], Omer Van der Biest[a]

[a]*Department of Metallurgy and Materials Engineering (MTM), Katholieke Universiteit Leuven, B-3001 Heverlee, Belgium*
[b]*State Key Laboratory of High Performance Ceramics and Superfine Microstructures, Shanghai Institute of Ceramics, Shanghai 200050, China*

Received 3 May 2012; received in revised form 26 May 2012; accepted 4 June 2012
Available online 12 June 2012

Abstract

Fully dense ZrB_2–20vol% SiC (ZS) ceramics were fabricated by self-made high purity ZrB_2 and SiC powders hot-pressing at 1900 °C/30 MPa. Their properties were compared with other ZS ceramics with the same nominal composition, but prepared by pressureless sintering, using low purity commercially available powders. The hot-pressed composites show superior hardness (17.82 GPa), elastic modulus (504 GPa), flexure strength (462 MPa at 25 °C and 463 MPa at 1300 °C in air), electrical conductivity ($7.68 \times 10^{-6}\ \Omega^{-1}\ m^{-1}$ at 25 °C), thermal conductivity (93.7 W/(m K) at 25 °C, 77.2 W/(m K) at 1200 °C) and a lower average thermal expansion coefficient ($6.66 \times 10^{-6}\ K^{-1}$ from 25 to 2000 °C) compared to the pressureless sintered materials. The improvement in these properties could be primarily explained by the decrease of impurities and second phase levels in hot pressed samples.

Keywords: A. Hot pressing; C. Mechanical properties; C. Thermal properties; D. Borides

1. Introduction

UHTCs, the acronym of ultra-high temperature ceramics, include the zirconium, hafnium and tantalum based borides, carbides, nitrides and their composites. All of them possess high melting points (near or above 3000 °C), high hardness, good chemical stability and relatively high strength at elevated temperatures. Another advantage of UHTCs is that their corresponding oxides also have high melting points (near or above 2000 °C) [1–3]. So UHTCs are expected to be used for thermal protection materials and sharp-leading-edge components in future high Mach (7–20 M) hypersonic flight, atmospheric re-entry vehicles as well as for rocket propulsion hardware. In the family of UHTCs, borides have relatively higher thermal conductivity, and ZrB_2 has the lowest theoretical density (6.09 g/cm^3) among the borides. Furthermore, the incorporation of SiC (normally 20% in volume) in ZrB_2 matrix significantly improves the oxidation resistance, strength and fracture toughness of monolithic ZrB_2 ceramics, so ZrB_2–20 vol% SiC (ZS) ceramics become the representative members in UHTCs [1,2]. For the intended applications, ZS ceramics have to be evaluated under the convective flows with high speed (over 7Mach), high temperature (>1600 °C) together with significant concentrations of molecular or dissociated oxygen [1,3].

In order to make ceramics suitable for the mentioned applications in extreme environments, apart from a high melting point, numerous mechanical and physical properties should also be satisfied [4]. Firstly, they should be strong enough at higher temperatures, i.e., excellent high temperature strength, which is an important aspect for evaluating the load-carrying capacity of ZS materials at the service temperatures. Secondly, they should exhibit excellent thermal–physical properties. As we know, high thermal conductivity of ceramics is helpful to reduce the temperature gradients and thermal stresses in the components induced by cooling down from high temperatures,

---

*Corresponding author. Tel.: +86 21 52411080; fax: +86 21 52413122.
**Corresponding author. Tel.: +32 16 321244; fax: +32 16 321992.
E-mail addresses: gjzhang@mail.sic.ac.cn (G.-J. Zhang), Jozef.Vleugels@mtm.kuleuven.be (J. Vleugels).

0272-8842/$36.00 © 2012 Elsevier Ltd and Techna Group S.r.l. All rights reserved.
http://dx.doi.org/10.1016/j.ceramint.2012.06.018

and thus beneficial to the thermal shock resistance of ZS ceramics. Therefore, comprehensive investigations of the properties of sintered ZrB_2–SiC ceramics and on effective methods to improve them are very important.

Most of the mechanical and physical properties of UHTCs are associated with and could be further tailored by the nature of starting powders, e.g., their particle sizes [5–7], morphologies [8] and purities [9,10]. Among these factors, the impurities in ZrB_2, especially for the oxygen impurity, attract more interests [1,11]. It will not only inhibit the densification behavior of ZS ceramics [11] but could decrease its high temperature strength [6] by the formation of glass phases as well. In this paper, high-purity ZrB_2 powder, synthesized by a boron/carbon thermal reduction method, was chosen as the starting material, and mechanical, thermal and electrical properties of hot pressed ZrB_2–20 vol% SiC ceramics from room to high temperature were systematically investigated. Data from the literature [12] were used for comparison and discussion.

2. Experimental procedures

The raw materials used were ZrB_2 powder provided by our group ($D_{50}=1.05$ μm, purity 98%, O 0.46%, C 0.1%, Hf 1.10%, others < 0.1%) and commercial alfa-SiC powders ($D_{50}=0.45$ μm, purity 98.5%, Changle Xinyuan Carborundum Micropowder Co. Ltd, Changle, China). Powder mixtures with compositions of 80 vol% ZrB_2 and 20 vol% SiC were mixed for 24 h in a polyethylene jar using acetone and Si_3N_4 balls, and dried through rotary evaporation. Hot pressing sintering was conducted for 1 h at 1900 °C with a pressure of 30 MPa using graphite dies in a flowing argon atmosphere, and the corresponding sample was marked as HP-ZS for simplicity. Another ZrB_2–20 vol% SiC ceramics (PLS-ZS) were used for a comparison [12], which were pressureless sintered at 2100 °C by commercial available ZrB_2 ($D_{50}=2.5$ μm, purity > 93.50%, Dandong Chemical Co. Ltd., Dandong, China) and SiC ($D_{50}=0.5$ μm) powders. In order to accelerate the pressureless densification process of PLS-ZS, 3 wt% C and 0.5 wt% B_4C were added as sintering aids. The details in the processing and properties of PLS-ZS have been reported elsewhere [12].

Vickers' hardness and indentation fracture toughness of HP-ZS and PLS-ZS were determined from the average of at least ten indents produced using a 5 Kg load, with 10 s hold, on a polished surface of the specimens. The toughness can be calculated by the following equations [13]:

$$K_{IC} = P\left[\pi\left(\frac{C_1+C_2}{4}\right)\right]^{-(3/2)}(\tan\beta)^{-1} \tag{1}$$

where, P is the indentation load, C_1 and C_2 are the measured diagonal crack lengths (m), and β is the angle constant (68°).

The flexure strength at room and high temperature was measured in three-point bending in flowing air, with bar dimensions of $3\times4\times36$ mm^3. The elastic modulus was obtained from the load–displacement curves as well as from an impulse excitation method.

Thermal expansion coefficient (TEC) of rectangular specimen ($4.3\times4.3\times25$ mm^3) was obtained using a dilatometer (Dil-402E, Netzsch, Selb, Germany) from room temperature to 2000 °C in argon. The final results were corrected by a standard graphite sample from Poco Graphite. Electrical conductivity measurement were carried out by a four-point probe method using samples with dimensions of $2\times2.5\times25$ mm^3 in the temperature range of 25–600 °C in argon. Four Cu probes (two inner current probes and two outer voltage probes) were fixed on the sample by silver paste. Thermal diffusivity (α) was measured on a carbon coated disk with a diameter of 10.7 mm and a thickness of 2 mm using a laser flash method from room temperature to 1200 °C in vacuum. The specific heat capacity (C_p) of ZS was mass-averaged using theoretical densities and nominal volume fractions, data from the NIST-JANAF tables for alfa-SiC (cr) and ZrB_2 (cr). The thermal conductivity (λ) is calculated based on the thermal diffusivities (α), heat capacities (C_p) and the measured density of ZS (ρ), according to the following equation:

$$\lambda = \alpha C_p \rho \tag{2}$$

3. Results and discussions

The polished and etched surfaces of HP-ZS and PLS-ZS ceramics are shown in Fig. 1a and b, and both of them reached a relative density of over 99% (Table 1). Benefiting from the finer starting powders, the assistance of the applied pressure and the relatively lower sintering temperature, the grain sizes of ZrB_2 (2.7 μm) and SiC (2.0 μm in length) in HP-ZS are obviously smaller than those in PLS-ZS, which are about 6.0 μm and 3.0 μm in length, respectively. The grain refinement leads to an increase of the number of grain boundaries in HP-ZS directly, and grain boundaries could pin dislocations induced by indentation. A substantially higher hardness was observed in HP-ZS (17.8 GPa) compared to that in PLS-ZS (14.7 GPa). Again, smaller grain size is also thought to be the main reason for the higher room temperature strength of HP-ZS (462 ± 47 MPa) compared to PLS-ZS (361 ± 44 MPa). Elastic modulus (E) is normally regarded as independent of the microstructure in ceramic, while E is higher in HP-ZS. The reason should be attributed to the additional phases in PLS-ZS, e.g., carbon, which has low modulus. Moreover, E calculated from bending test (for HP-ZS, 454 GPa) is significantly lower than that from the impulse excitation method (504 GPa) or the mixture rule (~490 GPa, considered $E_{ZrB_2}=500$ GPa and $E_{SiC}=450$ GPa), which implies an artifact exists in the former testing method. Alireza [5] reported that the fracture toughness (K_{IC}) decreased with the increase of SiC grain size in ZrB_2–SiC ceramics. However, the K_{IC} value of HP-ZS is actually lower than that of PLS-ZS in spite of the larger SiC grain

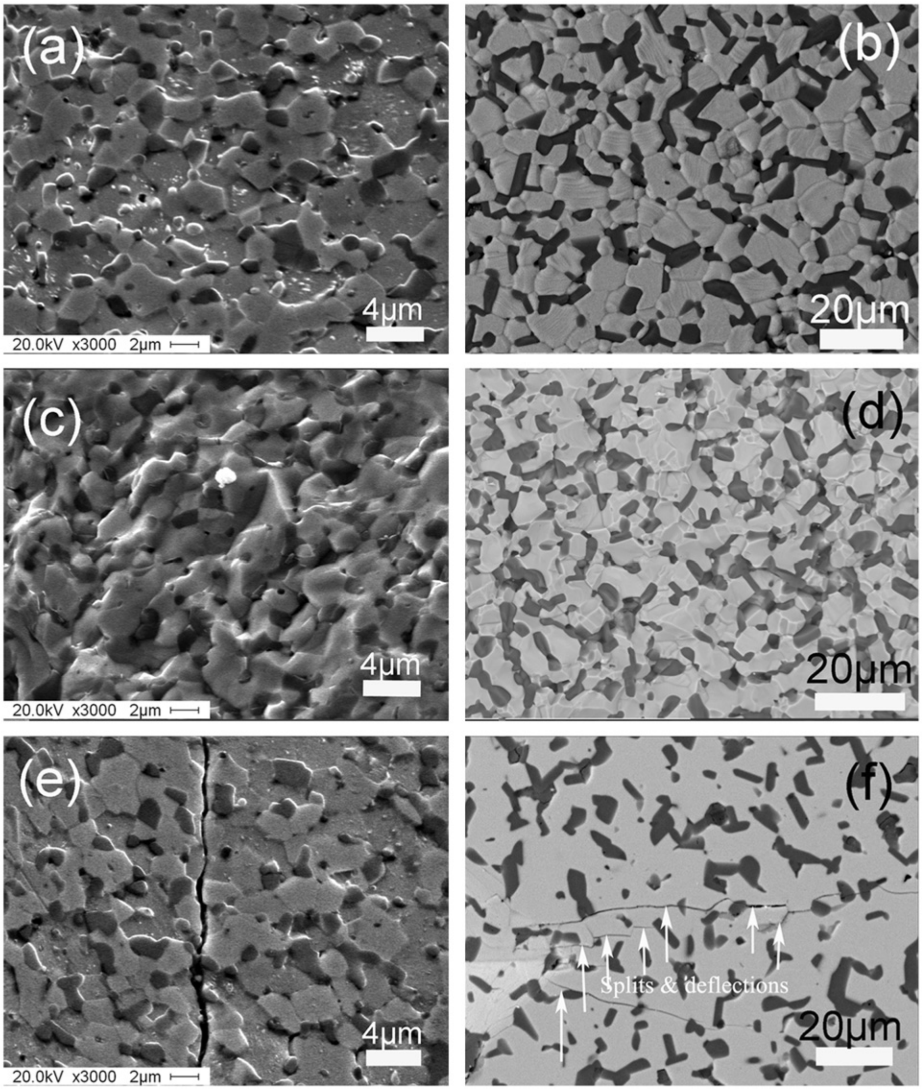

Fig. 1. The polished and etched surfaces of HP-ZS (a) and PLS-ZS (b) ceramics, (c) and (d) are the fracture surface of HP-ZS and PLS-ZS ceramics, (e) shows no obvious crack deflection in HP-ZS, while crack deflection and crack branching was found in PLS-ZS (f).

Table 1
Comparison of density and grain size between HP-ZS and PLS-ZS.

Properties	Units	HP-ZS	PLS-ZS
Density	g/cm^3	5.54	5.18
Open porosity	%	0.06	0.23
Relative density	%	> 99	99.3
Grain sizes			
ZrB_2	μm	2.7 ± 1.9	6.3 ± 3.1
Sic		Length ~2.0 Width ~1.3	Length ~6.0 Width ~3.0

size in PLS-ZS. The decrease of K_{IC} in HP-ZS is probably associated with its stronger grain boundary. As shown in Fig. 1c, the fracture of HP-ZS was predominantly intergranular, while a mixture of transgranular and intergranular fracture modes were found in PLS-ZS (Fig. 1d). Thus, compared to PLS-ZS (Fig. 1f), several mechanisms for toughening, such as crack deflection and bridging, were not operating in HP-ZS (Fig. 1e), which may explain its lower toughness (3.4 ± 0.5 MPa m$^{1/2}$) compared with PLS-ZS (4.0 ± 0.5 MPa m$^{1/2}$).

The strength increase of HP-ZS is more obvious at higher temperature, which is 478 ± 25 MPa for HP-ZS vs. 261 ± 45 MPa for PLS-ZS at 1200 °C. Increasing the test temperature to 1300 °C shows no clearly visible strength degradation of HP-ZS, and its fracture strength at 1300 °C (463 ± 40 MPa) in air is comparable to that at room temperature (462 ± 47 MPa). A glassy layer was found on the fracture surface (Fig. 2). The formation of glass phase is thought to be helpful for the crack healing on the tensile surface of the bars, and thus it is helpful to retain the strength of HP-ZS at 1300 °C. However, such enhancement is only available when the testing temperature is lower than the softening temperature of grain-boundary phase, and that is why the strength of HP-ZS at 1200 °C was predominantly higher than that of ceramics sintered from commercial powders with or without oxide additions (250–280 MPa [14] in Table 2).

Thermal strains ($\Delta L/L_0^{-1}$) and TEC of HP-ZS and PLS-ZS as a function of temperature are plotted in Fig. 3a and b. These thermal expansion curves could be well fitted by a third order polynomial below 1700 °C, similar to the results in other polycrystalline ceramics [15]. Nevertheless, above 1700 °C, the changes of thermal strains with temperature for HP-ZS seem to become linear. The average TEC of HP-ZS and PLS-ZS from 25 °C to 1200 °C was determined to be 6.09×10^{-6} and $6.99\times10^{-6}\,\mathrm{K}^{-1}$, respectively. Considering that TEC is partially affected by the average bonding strength of the specimen, the lower TEC in HP-ZS implies its bonding is stronger than that of PLS-ZS and sample listed in Table 2, which makes this material more resistant to thermal shock. The average TEC for HP-ZS from 25 °C to 2000 °C is $6.66\times10^{-6}\,\mathrm{K}^{-1}$, and TEC has been found to be proportional to the molar heat capacity [15]. Hence, TEC of ZS should approach a constant value for temperature over the Deby temperature based on the temperature dependence of its heat capacity. TEC of HP-ZS nearly keeps a constant below 1700 °C (Fig. 3a) as predicted. However, an obvious fluctuation and a tendency of decrease occurs when temperature is higher than 1700 °C. It could be inferred by a combination of several phenomenon, e.g., the grain sliding or partial creep of HP-ZS occurring at such a high temperature, since a small mechanical force needs to be applied on the sides of the specimen during TEC test. The current speculation of grain sliding has also been supported by several researches on high temperature creep and strength of ZS ceramics [6,16]. Anyway, the TEC of HP-ZS at 2000 °C is still

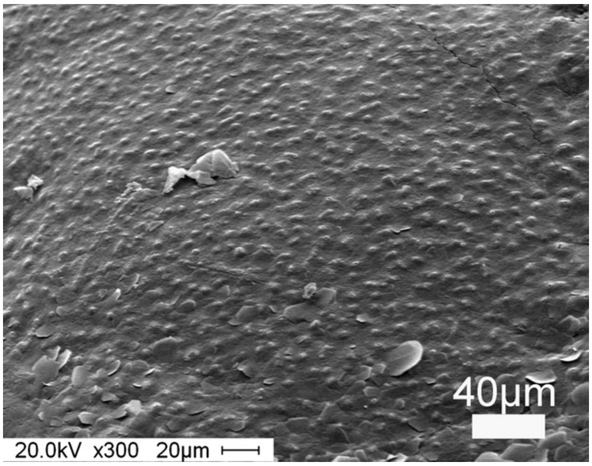

Fig. 2. The fractural surface of HP-ZS at 1300 °C.

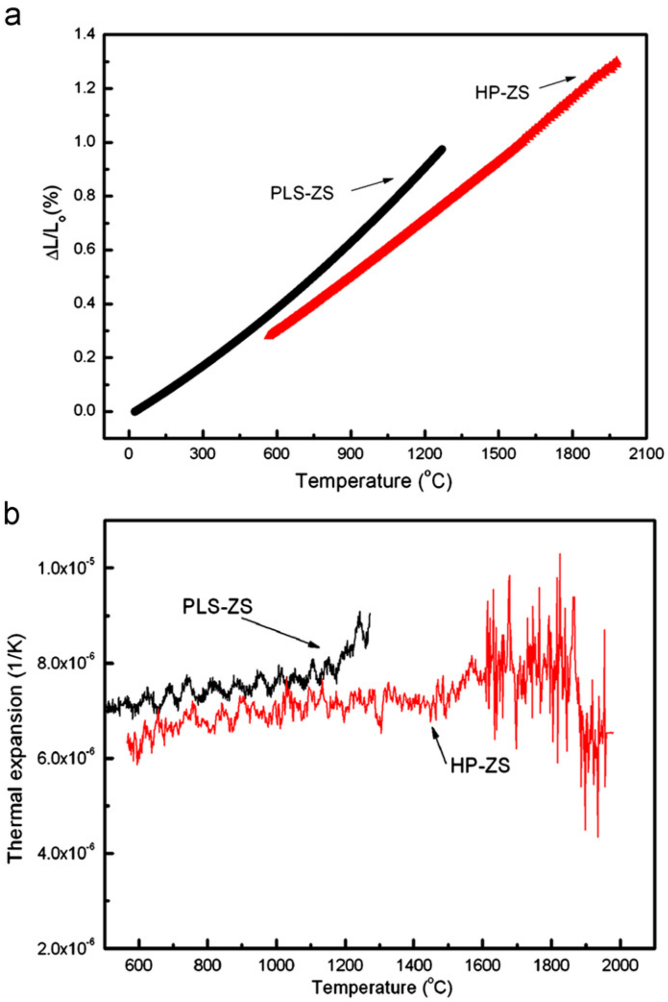

Fig. 3. Thermal expansion curves (a) and thermal expansion coefficients (b) of HP-ZS and PLS-ZS as a function of temperature.

Table 2
Comparison of mechanical and thermal–physical properties of HP-ZS, PLS-ZS and results from literature.

Materials	E (GPa)	Hv (GPa)	K_{IC} (MPa · $m^{1/2}$)	σ (MPa)		TEC ($10^{-6}\,\mathrm{K}^{-1}$) (25 – 1200 °C)	Electrical conductivity ($\Omega^{-1}\,m^{-1}$)	Thermal conductivity W/(m K)	
				25 °C	1200 °C			25 °C	1200 °C
HP-ZS	504	17.8	3.4 ± 0.2	462 ± 47	478 ± 25	6.09	7.68×10^{6}	93.7	77.2
PLS-ZS [12]	/	14.7	4.0 ± 0.5	361 ± 44	261 ± 45	6.99	7.51×10^{6}	94.1	62.3
ZrB_2–20% SiC-4Si_3N_4 [15]	/	14.6	/	730 ± 100	250 ± 10	7.45	6.67×10^{6}	/	/
ZrB_2–19% SiC–Si_3N_4–Y_2O_3–Al_2O_3 [15]	421	14.2	4.55 ± 0.1	710 ± 110	280 ± 20	7.39	6.25×10^{6}	/	/

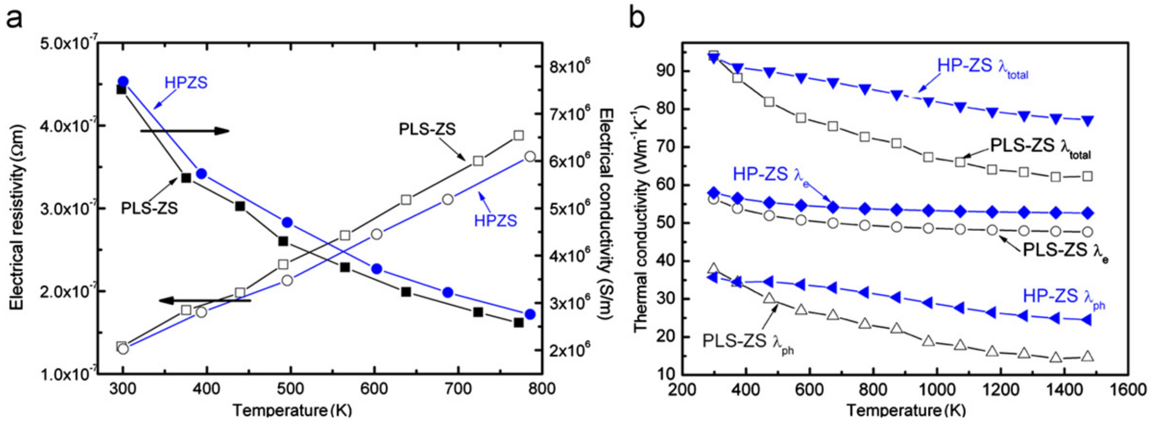

Fig. 4. Temperature dependence of electrical conductivity (a) and thermal conductivity (b) of HP-ZS and PLS-ZS, the thermal data shown for PLS-ZS are from literature [12].

positive, indicating that enough stiffness still retained at such a higher temperature.

The electrical conductivity (σ) of HP-ZS is higher than that of PLS-ZS at 25–500 °C, as shown in Fig. 4a. The reason could be explained by some additives with low electrical conductivity left in PLS-ZS, such as B_4C and ZrO_2. However, the differences are not obvious within this temperature range. At room temperature, the electrical conductivities of HP-ZS and PLS-ZS are 7.68×10^6 and $7.51\times10^6\ \Omega^{-1}\,m^{-1}$, respectively. They are higher than in a series of ZrB_2–SiC–ZrC ceramics with different compositions (0.9–$4.5\times10^6\ \Omega^{-1}\,m^{-1}$) [17], but lower than those of ZrB_2 ceramics with (10–30)vol% $ZrSi_2$ additions (9.6–$11.9\times10^6\ \Omega^{-1}\,m^{-1}$) [18], due to the existence of larger electrical resistivity of SiC phase. Generally, the electrical conductivity of HP-ZS and PLS-ZS ceramics decreases with the increasing temperature, indicating a metallic characteristic of ZS ceramics. The σ value of ZS ceramics mainly comes from the contribution of the electrons in the Zr 4d orbit, which makes the electronic density of states of ZrB_2 near the Fermi level larger than zero [19]. The temperature dependence of electrical resistivity of ZS ceramics can be fitted according to Eq. (3):

$$\rho(\mu\,\Omega\,m)=\rho_0(1-\beta(273.15-T)) \tag{3}$$

where ρ_0 is the electrical resistivity at 273.15 K ($\mu\,\Omega^{-1}\,m^{-1}$), T is the absolute temperature (K), and β is the temperature coefficient of resistivity (K^{-1}). The β value is very similar for HP-ZS and PLS-ZS, $4.2\times10^{-3}\,K^{-1}$ and $4.6\times10^{-3}\,K^{-1}$ respectively, slightly lower than for the ZS ceramics reported by Tye and Clougherty ($4.8\times10^{-3}\,K^{-1}$) [20].

The thermal conductivity (λ) comparisons of PLS-ZS and HP-ZS are shown in Fig. 4b. In general, λ decreases with increasing temperature, especially in the range from 300 K to 1200 K. Above this temperature, no remarkable change of λ was observed. At room temperature, $\lambda_{\text{HP-ZS}}$ (93.7 W/(m K)) and $\lambda_{\text{PLS-ZS}}$ (94.1 W/(m K)) are similar, but $\lambda_{\text{PLS-ZS}}$ decreases more quickly than $\lambda_{\text{HP-ZS}}$ when temperature increases. So $\lambda_{\text{PLS-ZS}}$ is lower than $\lambda_{\text{HP-ZS}}$ above 400 K. It is well established that at moderate temperature, when the contribution on thermal conductivity by photon could be neglected, the total thermal conductivity (λ_{total}) is equal to the sum of the contributions from electron (λ_{e}) and phonon (λ_{ph}) [21]:

$$\lambda_{total}=\lambda_e+\lambda_{ph} \tag{4}$$

According to Wiedemann and Franz Law, the ratio of λ_e and σ_e is proportional to Lorentz number (Eq. (5)) [21], so λ_e and λ_{ph} as a function of temperature could be calculated based on Eqs. (4) and (5) separately, as shown in Fig. 4b.

$$\frac{\lambda}{\sigma T}=L \tag{5}$$

where L (Lorentz number) is 2.443×10^{-8} ($J\,\Omega\,K^{-2}$) and T is the absolute temperature (K)

In both samples, the proportion of λ_e in λ_{total} is higher than that of λ_{ph} in all temperature ranges. From Fig. 4, λ_e is not very sensitive to the change of temperatures while λ_{ph} decreases with the increase of temperatures. Therefore, the contribution of λ_e in λ_{total} increases with temperature. It could also be found that lower $\lambda_{\text{PLS-ZS}}$ at higher temperatures is mainly a result of its lower λ_{ph} compared to that of $\lambda_{\text{HP-ZS}}$. λ_{ph} can be expressed as the product of bulk density of the sample, the velocity, and the mean free path of the phonon. The former two factors are considered as constants which are independent of temperature in present work. The average grain size in PLS-ZS is larger than that of HP-ZS. Increasing grain size means reducing the number of grain boundaries, so the mean free path for phonon should be larger in PLS-ZS than in HP-ZS. On the contrary, $\lambda_{\text{HP-ZS}}$ is larger than $\lambda_{\text{PLS-ZS}}$. The reason is that the scattering of phonon is supposed to be minimized in HP-ZS benefiting from the high purity starting ZrB_2 powders, i.e. without the formation of solid solution by incorporating impurities, and the lack of external phases. It shows that the thermal resistance at ZrB_2 or SiC/impurity boundary is more important than that at ZrB_2/SiC or ZrB_2/ZrB_2 based on the current results. In PLS-ZS, the impurities, carbon and boron carbide additions probably act as phonon scattering sites, which accelerate collision through phonon–phonon and phonon–lattice, especially at higher temperature. In return, the mean free path of phonon as well as the thermal conductivity of PLS-ZS decreased.

4. Conclusions

A ZrB_2–20 vol% SiC composite was fabricated by hot-pressing method using high purity ZrB_2 and SiC powders. The mechanical, thermal and electrical properties of the composite were comprehensively investigated and compared with those from pressureless sintered samples by commercial powders with low impurity. The strength of HP-ZS at 1200 °C in air is 478 ± 40 MPa, which is 1.86 times larger than that measured for PLS-ZS at the same temperature, and the thermal conductivity of HP-ZS at 1200 °C is as high as 77.2 W/(m K), significantly larger than that of PLS-ZS (62.3 W/(m K)). Based on the present results, by choosing high purity starting powders, the improved properties of ZS ceramics, especially for the high temperature strength and thermal conductivity, could be substantially realized.

Acknowledgments

Dr. Ji Zou thanks the Research Fund of K.U.Leuven for his post-doctoral fellowship (no. F+/11/006). This work was also financially supported by the NSFC (nos. 50632070 and 91026008), the Bilateral Project of NSFC-JSPS (no. 51111140017) and the Research Fund of K.U.Leuven under Project no. GOA/08/007. The Chinese Academy of Sciences Hundred Talents Program is gratefully acknowledged.

References

[1] W.G. Fahrenholtz, G.E. Hilmas, I.G. Talmy, J.A. Zaykoski, Refractory diborides of zirconium and hafnium, Journal of the American Ceramic Society 90 (2007) 1347–1364.

[2] K. Upadhya, J.M. Yang, W.P. Hoffman, Advanced materials for ultrahigh temperature structural applications above 2000 °C, American Ceramic Society Bulletin 76 (1997) 51–56.

[3] F. Monteverde, R. Savino, M.D. Fumo, Dynamic oxidation of ultra-high temperature ZrB_2–SiC under high enthalpy supersonic flows, Corrosion Science 53 (2011) 922–929.

[4] E. Wuchina, E. Opila, M. Opeka, W. Fahrenholtz, I. Talmy, UHTCs: ultra-high temperature ceramic materials for extreme environment applications, The Electrochemical Society Interface Winter (2007) 30–36.

[5] William G. Alireza Rezaie, Fahrenholtz, Greg E. Hilmas, Effect of hot pressing time and temperature on the microstructure and mechanical properties of ZrB_2–SiC, Journal of Materials Science 42 (2007) 2735–2744.

[6] P. Hu, Z. Wang, Flexural strength and fracture behavior of ZrB_2–SiC ultra-high temperature ceramic composites at 1800 °C, Journal of the European Ceramic Society 30 (2010) 1021–1026.

[7] S.C. Zhang, G.E. Hilmas, W.G. Fahrenholtz, Mechanical properties of sintered ZrB_2–SiC ceramics, Journal of the European Ceramic Society 31 (2011) 893–901.

[8] L. Silvestroni, D. Sciti, C. Melandri, S. Guicciardi, Toughened ZrB_2-based ceramics through SiC whisker or SiC chopped fiber additions, Journal of the European Ceramic Society 30 (2010) 2155–2164.

[9] L. Silvestroni, A. Bellosi, C. Melandri, D. Sciti, J.X. Liu, G.J. Zhang, Microstructure and properties of HfC and TaC-based ceramics obtained by ultrafine powder, Journal of the European Ceramic Society 31 (2011) 619–627.

[10] W.M. Guo, Z.G. Yang, G.J. Zhang, Effect of carbon impurities on hot-pressed ZrB_2–SiC ceramics, Journal of the American Ceramic Society 94 (2011) 3241–3244.

[11] S.C. Zhang, Greg E. Hilmas, William G. Fahrenholtz, Pressureless Sintering of ZrB_2–SiC ceramics, Journal of the American Ceramic Society 91 (2008) 26–32.

[12] H. Zhang, Y.J. Yan, Z.R. Huang, X.J. Liu, D.L. Jiang, Properties of ZrB_2–SiC ceramics by pressureless sintering, Journal of the American Ceramic Society 92 (2009) 1599–1602.

[13] A.G. Evans, E.A. Charles, Fracture toughness determinations by indentation, Journal of the American Ceramic Society 59 (1976) 371–372.

[14] F. Monteverde, S. Guicciardi, A. Bellosi, Advances in microstructure and mechanical properties of zirconium diboride based ceramics, Materials Science and Engineering A 346 (2003) 310–319.

[15] Rolf E. Hummel, in: Electronic Properties of Materials, fourth ed., Springer, New York, 2011.

[16] I.G. Talmy, J.A. Zaykoski, C.A. Martin, Flexural creep deformation of ZrB_2/SiC ceramics in oxidizing atmosphere, Journal of the American Ceramic Society 91 (2008) 1441–1447.

[17] S.Q. Guo, Y. Kagawa, T. Nishimura, D. Chung, J.M. Yang, Mechanical and physical behavior of spark plasma sintered ZrC–ZrB_2–SiC composites, Journal of the European Ceramic Society 28 (2008) 1279–1285.

[18] S.Q. Guo, Y. Kagawa, T. Nishimura, H. Tanaka, Pressureless sintering and physical properties of ZrB_2-based composites with $ZrSi_2$ additive, Scripta Materialia 58 (2008) 579–582.

[19] X.H. Zhang, X.G. Luo, J.C. Han, J.P. Li, W.B. Han, Electronic structure, elasticity and hardness of diborides of zirconium and hafnium: first principles calculations, Computational Materials Science 44 (2008) 411–421.

[20] R.P. Tye, E.V. Clougherty, The thermal and electrical conductivities of some electrically conducting compounds, in: Proceeding of the Fifth Symposium on Thermo-physical Properties, 1970, pp. 396–401.

[21] M.W. Barsoum, The $M_{N+1}AX_N$ phases: a new class of solids: thermodynamically stable nanolaminates, Progress in Solid State Chemistry 28 (2000) 201–281.